# Nanoherding: Plasma-Chemical Synthesis and Electric-Charge-Driven Self Organization of SiO₂ Nanodots

I. Levchenko,[‡,§] U. Cvelbar,[*,†] M. Modic,[†] G. Filipič,[†] X. X. Zhong,[∥] M. Mozetič,[†] and K. Ostrikov[‡,§,⊥]

†Jozef Stefan Institute, Jamova cesta 39, SI-1000 Ljubljana, Slovenia
‡CSIRO Materials Science and Engineering, P.O. Box 218, Lindfield, NSW 2070, Australia
§The University of Sydney, Sydney, NSW 2006, Australia
∥Shanghai Jiao Tong University, Shanghai 200240, People's Republic of China

Ⓢ *Supporting Information*

**ABSTRACT:** We report on the chemical synthesis of the arrays of silicon oxide nanodots and their self-organization on the surface via physical processes triggered by surface charges. The method based on chemically active oxygen plasma leads to the rearrangement of nanostructures and eventually to the formation of groups of nanodots. This behavior is explained in terms of the effect of electric field on the kinetics of surface processes. The direct measurements of the electric charges on the surface demonstrate that the charge correlates with the density and arrangement of nanodots within the array. Extensive numerical simulations support the proposed mechanism and prove a critical role of the electric charges in the self-organization. This simple and environment-friendly self-guided process could be used in the chemical synthesis of large arrays of nanodots on semiconducting surfaces for a variety of applications in catalysis, energy conversion and storage, photochemistry, environmental and biosensing, and several others.
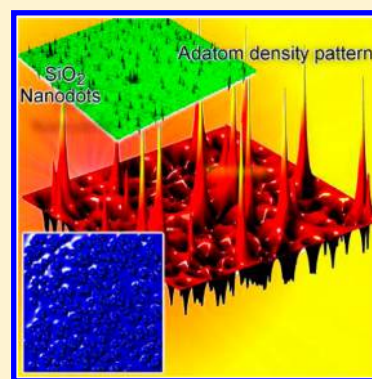
**SECTION:** Surfaces, Interfaces, Porous Materials, and Catalysis

Arranged and controlled patterns of low-dimensional nanostructures on semiconducting surfaces have recently been a subject of intense research efforts due to their unique size-dependent properties.[1−4] Large arrays of self-organized nanodots (NDs) are of particular interest, along with the arrays of highly ordered and densely packed silicon oxide NDs;[5,6] however, it is very challenging to identify and control the most effective driving forces for the ND self-organization. Electric forces have long been pursued as highly promising and easy-to-control driving forces for the arrangement of NDs on the surface.[7] Despite decades of intense experimental[8,9] and theoretical[10] studies, this control still remains elusive. Here we solve this problem by using chemically active low-temperature plasma, which ensures the chemical synthesis of NDs on surface and simultaneously guides the ND self-organization via physical processes triggered by surface charges. We demonstrate the effectiveness of this approach for silicon oxide NDs on silicon, one of the most commonly used ND systems.

The ordered arrays of silicon oxide (SiO₂) NDs chemically synthesized directly on the surface are of a special interest due to their importance for various applications such as biosensing,[11] photochemistry,[12] biomedical applications,[13] and others.[14] In these applications, the surface density and ordering of the NDs on a substrate surface are the key parameters, which determine performance of the devices.[15,16] Besides, the use of the silica ND arrays as a catalyst pattern for growing ordered forests of vertically aligned carbon nanotubes requires a very high level of process controllability.[17] High-temperature silicon oxidation in atmospheric-pressure oxygen-enriched environment results in SiO₂ NDs with many structural defects, which are not tolerated in the electronic and photonic devices. Moreover, thermal oxidation is not effective in controlling ND size distribution, surface density, and ordering on the surface. Other possible methods such as nanosphere lithography and liquid-phase deposition are very expensive and difficult to control.[18] The Stranski−Krastanow growth is also a very complex process with a very low controllability.[19] Recently, it was demonstrated that inductively coupled radio frequency (ICRF) plasmas are very effective for the self-organized synthesis of SiO₂ NDs at very low (not exceeding 100 °C) temperatures, thus ensuring fabrication of the defect-free silicon−silica interfaces.[20] The plasma-based methods of silicon oxidation and synthesizing SiO₂ ND patterns offer a promise for better controllability, mainly due to the effects of the electric charges and fields at the plasma-surface interface. Although the idea of controlling self-organization of the ND array formation by surface charges on the surface was proposed, there has been no convincing experimental demonstration and numerical modeling that can explain these phenomena.[21−23]

In our previous work, we have reported on the kinetic of SiO₂ NDs formation on the plasma-exposed surfaces. In this

work, we demonstrate that the electric field-induced effects, and specifically the electric charges on the surface, control self-organization of large patterns of $SiO_2$ NDs chemically synthesized on a Si surface. Specifically, we show that the number of NDs on the surface as well as their density strongly correlate with the electric charges accumulated on the substrate. Hence, the discharge parameters such as RF power, electron energy, and plasma density, which directly influence the surface charges via the balance of electron and ion fluxes, can be used to control the most important characteristics of the $SiO_2$ ND array. Therefore, controlling the surface charge (potential) via the plasma parameters may be a viable method for structuring self-organized ND arrays.

Figure 1 shows the results of the AFM measurements of several samples with the arrays of $SiO_2$ NDs formed in 15, 25,
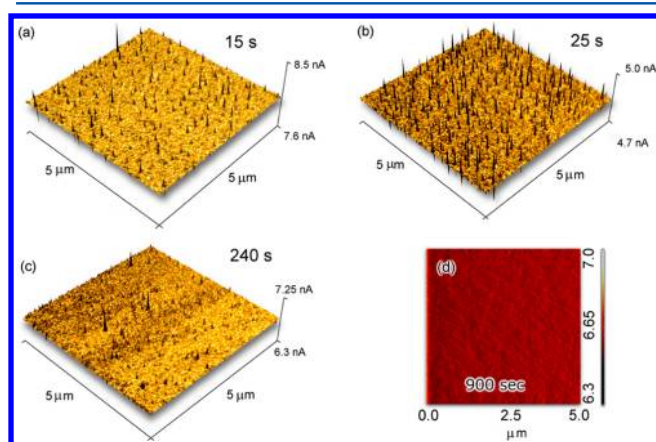


**Figure 1.** (a–d) Typical AFM images of $SiO_2$ nanodots synthesized on a Si surface in chemically active oxygen plasmas for 15, 25, 240, and 900 s, respectively. The surface density of the nanodots increases with time, and the highest nanodot density was found for the 25 s process. (See Figure 2 for the time dependence of the nanodot number.) At 900 s, a continuous film was formed.

240, and 900 s. (See also Figure S1 in the Supporting Information.) These images show that the highest ND density was reached at 20–25 s into the process. Afterward, the surface density of the NDs continuously decreased, eventually resulting in the formation of a continuous film with the thickness reaching ~50 nm, that is, equal to the height of NDs at the moment of the layer formation. Figure 2a,b shows the ND array characteristics calculated by the data obtained from AFM characterization. From these graphs, one can see that initially the number of NDs increases but then drops down abruptly by a factor of 20 after 20–25 s into the process. All of these parameters experience a strong jump by a factor of ~10. Besides, it can be noticed that the ND height decreases strongly after 70–100 s.

The results of the surface electric potential measurements are shown in Figure 2c. After switching on the RF discharge, the potential of the sample surface immediately jumps up to 20 V and then increases further to 40 V. After that, it starts decreasing. (Note that the discharge is still on and the discharge power was not changed during the process, that is, during 1000 s.) After 250 s into the process, the electric charge drops to nearly zero. Note that the number of NDs on the surface as well as the sizes of NDs do not change after 50–100 s. A strong correlation with the graphs shown in Figure 2a,b can be noticed, with the maximum surface potential detected at 25 s

after the start of the process, that is, at the time point when the highest surface density of the NDs was registered.

One more interesting observation is the grouping of the NDs. As it was noticed, the initially uniform distribution of the NDs on the surface was disturbed after 50–100 s, and the dots started to form linear and area groups, that is, lines and clusters of NDs. (These measurements were made mainly using SEM images due to low resolution of the lateral AFM measurements.) To characterize the area grouping, we have plotted a graph of scattering of the distances between the NDs. To generate this graph, we measured the distances between all NDs on the surface and then plotted the number of distances in some "distance slot" versus the mean distance of this slot. For example, setting a slot of 0.2 $\mu$m would give 25 slots for a 5 $\mu$m substrate size, with the mean slot distances being of 0.1, 0.3, and 0.5 $\mu$m and so on. The graph is shown in Figure 2d. It is clear that if all NDs are distributed uniformly, then the graph would show a peak at the half of the substrate size, that is, 2.5 $\mu$m in this case. If there is any grouping with some characteristic size, then the graph will also show a peak at that size. From this Figure, one can clearly see that the graph shows the presence of groups of NDs with the mean size 0.25 $\mu$m (the first peak at 0.25 $\mu$m). The examples (SEM and AFM images) are shown in Figure 2e,f (area grouping) and Figure 2g (line grouping). In contrast with the line grouping, which is clearly visible in Figure 2g, the area grouping is not so clear. This is why we have used a dedicated data postprocessing to examine the area grouping of the NDs on the surface.

Now an interpretation and discussion of the results will be presented. As previously mentioned, the most interesting observations are: (i) a strong correlation between the dependence of the number of NDs on time and the dependence of the surface potential on time (charge/density correlation) and (ii) plasma-specific area and line grouping of the NDs. Therefore, we will start from considering the most remarkable trends of the process and eventually will try to find a plausible mechanism to explain the charge/density correlation and ND grouping during the chemical synthesis of the NDs on the plasma-exposed charged surface.

The separate stages of this process are illustrated on Figure S2 in the Supporting Information. At the beginning of the process, a flux of the reactive oxygen species (atoms, molecules, and ions) onto the silicon surface causes the initial nucleation of the NDs. The initial nucleation most likely proceeds on the nanohillocks, that is, small (not exceeding several nanometers) humps present on the nontreated silicon surface.[20] The number of NDs increases due to the progressive increase in the number of oxidized nanohillocks, and eventually, the surface density of the NDs reaches the maximum at 25 s. After that, the number of NDs cannot increase due to the absence of the available nucleation sites, and the NDs grow in size, increasing their height and volume. When the interdot distance becomes small, coalescence starts, and hence, the number of NDs decreases abruptly. Eventually, a continuous layer is formed.

However, this classical scenario should be modified to explain our striking observations, namely, the charge/density correlation and ND grouping. Indeed, the maximum surface charge corresponds to the maximum number of NDs, which happens when all available nanohillocks are saturated. This means that the conditions of the electric charge accumulation strongly depend on the surface processes that accompany chemical synthesis of the NDs and the formation of the array. Therefore, to explain the experimental results and to find how
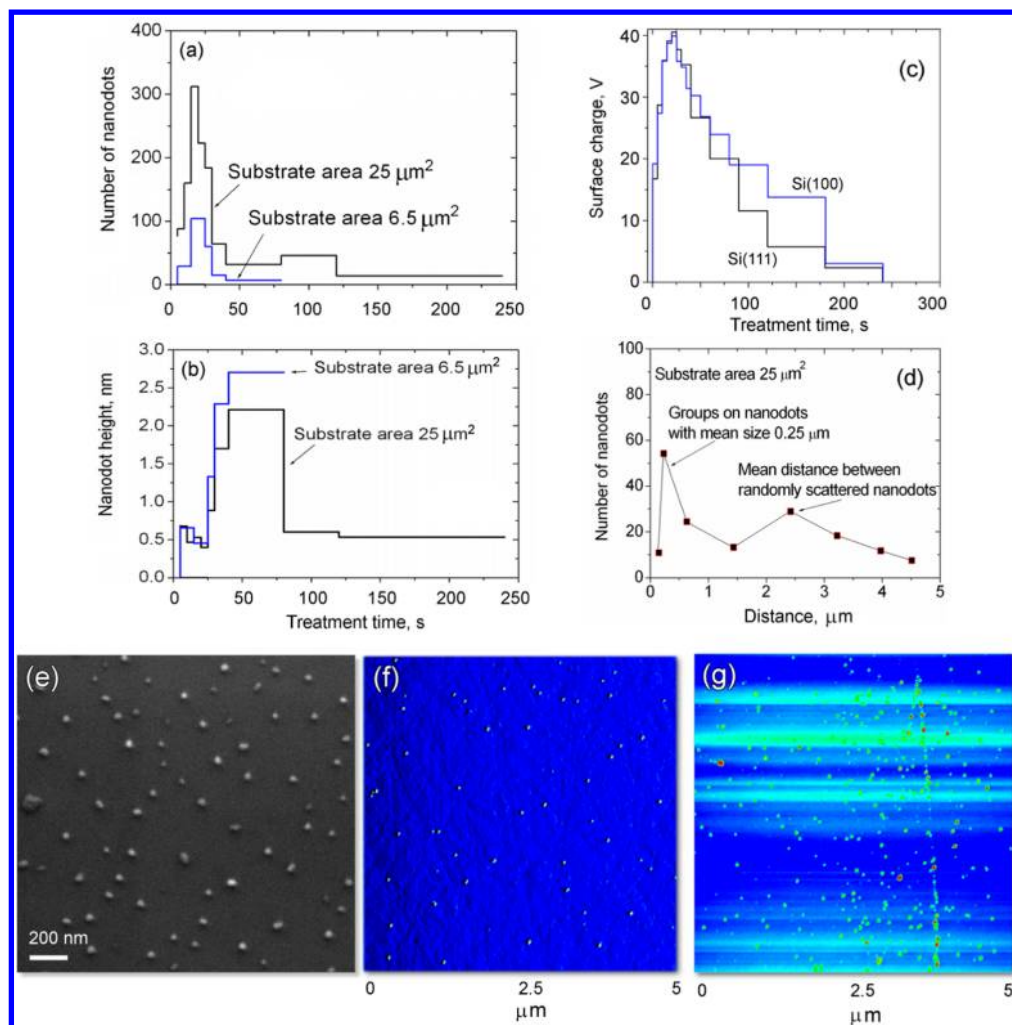
**Figure 2.** (a) Dependence of the number of nanodots on two substrates on the process time. Initial growth is followed by an abrupt decrease after 25 s into the process. (b) Dependence of the nanodot height on two substrates on the process time. (c) Dependence of the electric potential of the sample surface on treatment time for Si(100) and Si(111) surfaces. The maximum surface potential corresponds to the maximum number of nanodots, as shown in panel a. No significant difference between Si(100) and Si(111) is noticeable. (d) Scattering of distances between nanodots. Two clear peaks may be noticed, one at 2.5 μm, which corresponds to the uniform distribution of the nanodots, and one at 0.4 μm, which is attributed to the presence of the groups of nanodots. (e−g) SEM and AFM images of the nanodot pattern with the area (e,f) and line (g) grouping. Process parameters: pressure 100 Pa, current to the substrate 190 mA.

to use them to control the organization in the ND arrays, we should find out what happens on the surface at the moment of the nanohillocks saturation.

It is quite natural to assume that the electric-field-induced surface diffusion could be the main phenomenon responsible for the charge/density correlation and the change in the array formation behavior at the moment of saturation. Indeed, in the internanodot space (mean distance of ∼1 μm, surface potential of ∼40 V), the electric field can reach ∼$4 \times 10^7$ V × m$^{-1}$. Another estimate, which takes into account the ND size and curvature, gives an even higher value of ∼$10^8$ V × m$^{-1}$.

To support our assumption about the leading role of electric charges on the surface in the formation of ND groups, we have used extensive numerical simulations of the ND array formation in the plasma environment. A simulation of the diffusion-dependent growth on a real surface requires a complex model incorporating a large number of surface processes.[24] Here we have used a model based on a classical formulation of surface diffusion with a set of the experimentally measured microscopic parameters to increase the accuracy of

simulation. The following surface processes have been taken into account: surface diffusion of adsorbed atoms about surface areas between the NDs, evaporation from the silicon substrate and surfaces of NDs, attachment of the adsorbed atoms to the borders of the NDs, and supply of reactive oxygen atoms from the plasma to the surface. This model was used to simulate the growth of NDs and formation of the ND array on the plasma-exposed surface, under conditions of the accumulation of electric charges. More detail on the model can be found in the Supporting Information and in our previous publications.[25]

The results of calculations are shown in Figure 3. First, we have simulated the nucleation and initial stages of the ND formation, which demonstrate an increase in the number of NDs in the array. In this stage, we have used the experimentally obtained array characteristics (density of NDs on the surface and their size distribution) to adjust the simulation parameters in such a way to obtain a realistic array configuration. After reproducing the experimentally proven charge−time behavior, we have simulated the ND array formation on the charged surface. Our calculations have demonstrated that the strongest
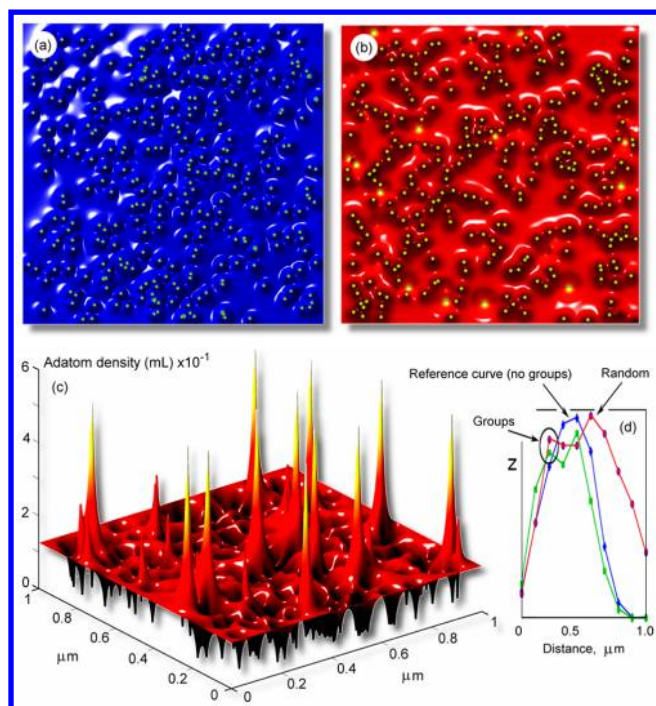
683

dx.doi.org/10.1021/jz400092m | *J. Phys. Chem. Lett.* 2013, 4, 681−686

**Figure 3.** Results of the numerical simulation of nanodot array formation on the Si surface exposed to chemically active plasma. (a) Calculated distribution of the electric field in the simulated pattern of nanodots; (b) half-tone visualization of adatom density on the silicon surface; and (c) 3D visualization of the nanodot pattern and adatom density profile on the silicon surface. Pattern size is $1 \times 1$ $\mu$m. (d) Calculated graph illustrating scattering of distances between the nanodots. The reference curve with one peak corresponds to the randomly distributed nanodot array, and two other curves show additional peaks at 0.25 $\mu$m corresponding to the nanodot groups.

electric field gradient is observed along the lines connecting the closest NDs. The calculations made using the first-principles molecular dynamics (MD) technique, along with the direct

experiments, have shown that the electric field affects the diffusion of adsorbed atoms on the surfaces due to the change in the diffusion activation energy,[26−28] which is mainly influenced by the electric field through the polarization-related effects.[29,30] Figure 3a illustrates the simulated ND pattern in the stage of the maximum ND number, with a half-tone representation of the electric field in the pattern. Figure 3b shows a half-tone visualization of the adatom density on the silicon surface. To better represent the simulation results, we have also made a 3D-visualization of the ND pattern and adatom density on the surface (Figure 3c). In this image, vertical humps between the NDs represent a field of adatom density (shown not to scale).

During these simulations, we have observed that indeed the electric charge of the plasma-exposed surface was continuously increasing due to the electron and ion fluxes from the plasma to the substrate surface. In the growth stages when the experiment shows the maximum number of the NDs on the surface and the maximum heights of the NDs, the calculated strength of the electric field at NDs of 3−5 nm reached the value above the threshold for the electron field emission ($10^8$ to $10^9$ V × m$^{-1}$). After that, an intense charge leakage from the surfaces of the NDs started, resulting in the effective "release" of the electric charge accumulated on the surface. During the next stages, that is, coalescence followed by the formation of a continuous layer, the NDs are still present on the surface, together with the natural irregularities of the silica layer. They provide the effective charge release from the surface, thus preventing any further charge accumulation. Therefore, we have incorporated a charge release factor (after 25 s into the process) into the model to achieve a better consistency in the charge behavior with time.

Our simulations involving the above effects have shown that the fluxes of adsorbed atoms on the substrate surface are the strongest between the adjacent NDs. Hence, the surface of the ND facing its nearest neighbor will receive the strongest flux of the material, and thus a preferential growth of the NDs will occur in the direction of the neighbor. Depending on the
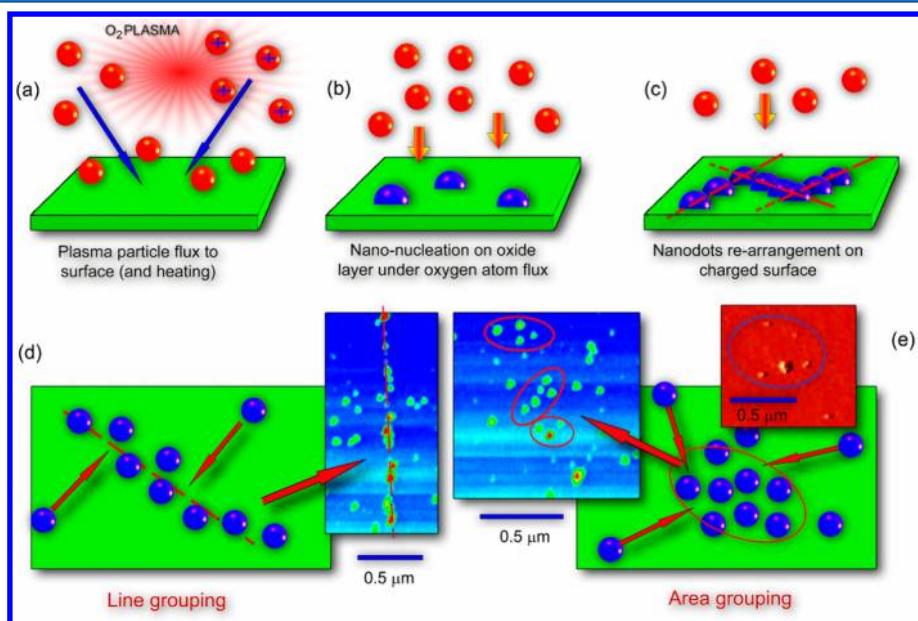


**Figure 4.** Grouping of SiO$_2$ nanodots on a Si surface exposed to chemically active oxygen plasmas. (a,b) nucleation and growth of the initial nanodot ensemble; (c,d) arrangement into lines (AFM image in inset); and (e) area grouping (AFM images in insets).

specific configuration of the NDs in the local zone of the array, this will lead to the line or area grouping found in our experiments (Figure 4). Indeed, the calculated graph of scattering of distances between the NDs in the simulated pattern (Figure 3d) shows the two peaks corresponding to the uniform distribution of the NDs and groups of NDs. Note that the scattering graph shown in Figure 3 cannot detect the line grouping separately of the area grouping; this may require the development of dedicated statistical methods for the identification.

One more important point is the controllability of self-organization on the plasma-exposed surfaces. Our experiments have shown that an effective self-organization occurs under conditions typical for the low-temperature plasma synthesis, that is, when the substrate surface contacting with the plasma acquires a significant electric potential. This potential originates from the electric charges accumulated on the surface due to a strong electron flux from the plasma-surface sheath. Because the electric charge on the surface is the main driving force of the self-organization, the controllability of the grouping should be attributed to the plasma parameter directly influencing the surface charge, that is, the electron energy. (See the Supporting Information where the ion and electron fluxes are discussed.) Indeed, the experiments conducted in plasma with significantly lower electron energy have demonstrated apparently lower level of the self-organization.

To conclude, we have reported the results of the experimental and numerical studies on the synthesis of the arrays of silica NDs on Si(100) and Si(111) surfaces exposed to the ICRF chemically active oxygen plasmas and simultaneous self-organization of these arrays via physical processes triggered by electric charges accumulated on the surface. The experimental results have demonstrated that the electric charge on the surface correlates with the density of the NDs and influences the array behavior. Moreover, we have found that the NDs tend to form areas with the increased density, namely, the area and linear groups. This phenomenon can be termed *nanoherding* of NDs on the surface. The surface charge triggers and guides the self-organization of NDs, which change behavior when closer to their neighbors with a tendency to merge. On the basis of the experimental results, we have proposed a mechanism of the ND array behavior based on the effect of the electric field on the surface in the rearrangement of the NDs within the array. To confirm this mechanism, we have developed a model and conducted extensive numerical simulations, which have confirmed the proposed mechanism and have proven a critical role of the electric charges in the behavior discovered. This process is essentially self-organized and could be useful for the development of new, self-organization-based techniques for the devices based on large-area ND arrays that require controlled ND alignment or grouping on the surface.

## ■ EXPERIMENTAL SECTION

The patterns of $SiO_2$ NDs were synthesized in the radio frequency (RF) chemically active oxygen plasma. The RF generator operating at 27.12 MHz was connected to the coil installed over the Pyrex glass chamber (tube of 10 cm in diameter and ~30 cm in length). The gas supply and pumping system maintained the gas pressure in the range of 10 to 100 Pa. A Si substrate was placed on the sample holder, which could be electrically biased by connecting to the RF circuit or disconnected from the RF circuit to maintain the floating

potential with respect to the plasma bulk. A measurement system capable of determining the electron temperature and the ion density in the plasma using a double Langmuir probe installed at the position of the sample was also used.[31] On the basis of these measurements, the plasma-surface sheath thickness and the current density to the surface were calculated.[32] Also, a custom-designed fiber optics catalytic probe was used to measure the density of the neutral oxygen species.[33]

Initially, silicon substrates were cleaned in ultrasound bath in acetone and ethanol for 5 and 10 min, respectively, and then dried using compressed nitrogen. Finally, the samples were installed on the sample holder of the vacuum chamber and exposed to the Ar atmosphere for several minutes. During the process, the electron energy was maintained in the range of 2–10 eV, ion density −(1 to 2.5) × $10^{16}$ m$^{-3}$, and density of neutral oxygen atoms −(1.0 to 2.5) × $10^{21}$ m$^{-3}$. The measured floating bias of the substrate was negative in the range of 10−15 V. The RF generator had a maximum power of 1 kW, and the RF bias was −100 V at the maximum RF power.

The RF coil was air-cooled during the process. The average temperature of the substrate surface was measured using an IR camera installed on the glass chamber. The samples used were Si wafers (Sigma Aldrich) of thickness 0.5 mm, cut into pieces of ~100 mm$^2$. Both (100) and (111) silicon surfaces were used in the experiments. No special catalysts were deposited on the substrate surface prior to the ND growth. A detailed schematic of the experimental setup is shown in Figure S3 in the Supporting Information.

The structure of the samples was analyzed using scanning electron microscopy (SEM) and atomic force microscopy (AFM) techniques. Besides, the electric potential of the sample surface was measured after the plasma process using TREK Kelvin probe. The Kelvin probe measurements with resolution ±1 V were noncontact from 2 mm distance. SEM and AFM data were used to calculate the geometrical characteristics of the ND pattern, namely, the dependence of the number of NDs, ND height, ND surface area, and ND volume on the process time. Also, the scattering of the distances between NDs was calculated using AFM data of 20 randomly selected sample surface areas of 6.5 $\mu m^2$ and NT-MDT software.

## ■ ASSOCIATED CONTENT

**Ⓢ Supporting Information**
High-resolution AFM measurements, schematic of the nanodot array formation, details of the model and simulations, and schematic of the experimental setup. This material is available free of charge via the Internet at http://pubs.acs.org.

## ■ AUTHOR INFORMATION

**Corresponding Author**
*E-mail: uros.cvelbar@ijs.si.
**Notes**
The authors declare no competing financial interest.
⊥E-mail: Kostya.Ostrikov@csiro.au.

## ■ ACKNOWLEDGMENTS

    

## ■ REFERENCES

(1) Liu, R.; Lee, S. B. MnO$_2$/Poly(3,4-ethylenedioxythiophene) Coaxial Nanowires by One-Step Coelectrodeposition for Electrochemical Energy Storage. *J. Am. Chem. Soc.* **2008**, *130*, 2942–2943.

(2) Zhang, J. Z. Understanding the Growth of Metal Oxide Nanostructures. *J. Phys. Chem. Lett.* **2012**, *3*, 2920–2921.

(3) Hetsch, F.; Xu, X.; Wang, H.; Kershaw, S. V.; Rogach, A. L. Semiconductor Nanocrystal Quantum Dots as Solar Cell Components and Photosensitizers: Material, Charge Transfer, and Separation Aspects of Some Device Topologies. *J. Phys. Chem. Lett.* **2011**, *2*, 1879–1887.

(4) Ueno, K.; Takabatake, S.; Nishijima, Y.; Mizeikis, V.; Yokota, Y.; Misawa, H. Nanogap-Assisted Surface Plasmon Nanolithography. *J. Phys. Chem. Lett.* **2010**, *1*, 657–662.

(5) Xu, J.; Hong, S. W.; Gu, W.; Lee, K. Y.; Kuo, D. S.; Xiao, S.; Russell, T. P. Fabrication of Silicon Oxide Nanodots with an Areal Density Beyond 1 Teradots Inch$^{-2}$. *Adv. Mater.* **2011**, *23*, 5755–5761.

(6) Park, S.; Kim, B.; Wang, J.-Y.; Russell, T. P. Fabrication of Highly Ordered Silicon Oxide Dots and Stripes From Block Copolymer Thin Films. *Adv. Mater.* **2008**, *20*, 681–685.

(7) Grzelczak, M.; Vermant, J.; Furst, E. M.; Liz-Marzan, L. M. Directed Self-Assembly of Nanoparticles. *ACS Nano* **2010**, *4*, 3591–3605.

(8) Tuten, B. T.; Chao, D.; Lyon, C. K.; Berda, E. B. Single-Chain Polymer Nanoparticles via Reversible Disulfide Bridges. *Polym. Chem* **2012**, *3*, 3068–3071.

(9) Appel, E. A.; Dyson, J.; Barrio, J.; Walsh, Z.; Scherman, O. A. Formation of Single-Chain Polymer Nanoparticles in Water Through Host–Guest Interactions. *Angew. Chem., Int. Ed.* **2012**, *51*, 4185–4189.

(10) Sinyagin, A. Y.; Belov, A.; Tang, Z.; Kotov, N. A. Monte Carlo Computer Simulation of Chain Formation From Nanoparticles. *J. Phys. Chem. B* **2006**, *110*, 7500–7507.

(11) Piao, Y.; Burns, A.; Kim, J.; Wiesner, U.; Hyeon, T. Design and Fabrication of Silica-Based Nanostructured Particle Systems for Nanomedicine Applications. *Adv. Funct. Mater.* **2008**, *18*, 1–14.

(12) Gratzel, M. Dye-Sensitized Solar Cells. *J. Photochem. Photobiol., C* **2003**, *4*, 145–153.

(13) Qhobosheane, M.; Zhang, P.; Tan, W. Assembly of Silica Nanoparticles for Two-Dimensional Nanomaterials. *J. Nanosci. Nanotechnol.* **2004**, *4*, 635–640.

(14) Luna-Lopez, A.; Aceves-Mijares, M.; Malik, O. Optical and Electrical Properties of Silicon Rich Oxide Films for Optical Sensors. *Sens. Actuators, A* **2006**, *132*, 278–282.

(15) Roczen, M.; Schade, M.; Malguth, E.; Callsen, G.; Barthel, T.; Gref, O.; Toffinger, J. A.; Schopke, A.; Schmidt, M.; Leipner, H. S.; et al. Structural Investigations of Silicon Nanostructures Grown by Self-Organized Island Formation for Photovoltaic Applications. *Appl. Phys. A: Mater. Sci. Process.* **2012**, *108*, 719–726.

(16) Caruge, J. M.; Halperrt, J. E.; Wood, V.; Bulovic, V.; Bawend, M. G. Colloidal Quantum-Dot Light-Emitting Diodes with Metal-Oxide Charge Transport Layers. *Nat. Photon.* **2008**, *2*, 247–250.

(17) Takagi, D.; Hibino, H.; Suzuki, S.; Kobayashi, Y.; Homma, Y. Carbon Nanotube Growth From Semiconductor Nanoparticles. *Nano Lett.* **2007**, *7*, 2272–2275.

(18) Kim, K. S.; Roh, Y. Selective Growth Of The Silicon-Oxide Nanodot Array Using Nanosphere Lithography and Liquid-Phase Deposition. *IEEE Trans. Nanotechnol.* **2010**, *9*, 361–366.

(19) Baskaran, A.; Smereka, P. Mechanisms of Stranski-Krastanov Growth. *J. Appl. Phys.* **2012**, *111*, 044321.

(20) Levchenko, I.; Cvelbar, U.; Ostrikov, K. Kinetics of the Initial Stage of Silicon Surface Oxidation: Deal–Grove or Surface Nucleation? *Appl. Phys. Lett.* **2009**, *95*, 021502.

(21) Arnoult, G.; Belmonte, T.; Kosior, F.; Dossot, M.; Henrion, G. On the Origin of Self-Organization of SiO$_2$ Nanodots Deposited by CVD Enhanced by Atmospheric Pressure Remote Microplasma. *J. Phys. D: Appl. Phys.* **2011**, *44*, 174022.

(22) Kumar, P. Directed Self-Assembly: Expectations and Achievements. *Nanoscale Res. Lett.* **2010**, *5*, 1367–1376.

(23) Lugomer, S.; Zolnai, Z.; Tóth, A. L.; Bársony, I. Self-Organization of Silica Nano-Particles Induced by the Ion Beam. *Phys. Status Solidi C* **2011**, *8*, 2858–2861.

(24) Levchenko, I.; Ostrikov, K.; Diwan, K.; Mariotti, D. Plasma-Driven Self-Organization of Ni Nanodot Arrays on Si(100). *Appl. Phys. Lett.* **2008**, *93*, 183102.

(25) Levchenko, I.; Ostrikov, K. Nanostructures of Various Dimensionalities From Plasma and Neutral Fluxes. *J. Phys. D.: Appl. Phys.* **2007**, *40*, 2308–2319.

(26) Kobayashi, A.; Grey, F.; Snyder, E.; Aono, M. Spatially Anisotropic Atom Extraction Around Defects on Si(001) Using a STM. *Phys. Rev. B* **1994**, *49*, 8067–8070.

(27) Kawai, T.; Watanabe, K. Diffusion of a Si Adatom on the Si(100) Surface in an Electric Field. *Surf. Sci.* **1996**, *357*, 830–834.

(28) Kandel, D.; Kaxiras, E. Microscopic Theory of Electromigration on Semiconductor Surfaces. *Phys. Rev. Lett.* **1996**, *76*, 1114–1117.

(29) Mattsson, T. R.; Swartzentruber, B. S.; Stumpf, R.; Feibelman, P. J. Electric Field Effects on Surface Dynamics: Si ad-Dimer Diffusion and Rotation on Si(001). *Surf. Sci.* **2003**, *536*, 121–129.

(30) Neyts, E. C.; Duin, A. C.; Bogaerts, A. Insights in the Plasma-Assisted Growth of Carbon Nanotubes Through Atomic Scale Simulations: effect of electric field. *J. Am. Chem. Soc.* **2012**, *134*, 1256–1260.

(31) Keidar, M.; Beilis, I. I. Sheath and Boundary Conditions for Plasma Simulations of a Hall Thruster Discharge with Magnetic Lenses. *Appl. Phys. Lett.* **2009**, *94*, 191501.

(32) Keidar, M.; Waas, A. M. On the Conditions of Carbon Nanotube Growth in the arc Discharge. *Nanotechnology* **2004**, *15*, 1571–1575.

(33) Cvelbar, U.; Mozetic, M.; Poberaj, I.; Babic, D.; Ricard, A. Characterization of Hydrogen Plasma with a Fiber Optics Catalytic Probe. *Thin Solid Films* **2005**, *475*, 12–16.